

Thermal design of air cooled condenser of a solar adsorption refrigerator

Amar Rouag¹✉, Adel Benchabane¹, Adnane Labeled², Nora Boultif¹

1 Laboratoire de Génie Énergétique et Matériaux (LGEM), Université de Biskra, B.P. 145 R.P. 07000, Biskra, Algeria

2 Laboratoire de Génie Mécanique (LGM), Université de Biskra, B.P. 145 R.P. 07000, Biskra, Algeria

Received 01 March 2015

Revised 26 March 2016

Accepted 27 March 2016

Published online: 30 March 2016

Keywords

Solar adsorption refrigerator

Condenser

LMTD

Sizing

Free convection

Forced convection

Abstract: The objective of this paper is to study the design of a condenser of a solar adsorption refrigerator which will be tested in the region of Biskra (Algeria). The LMTD (log mean temperature difference) method is used to calculate the size of the condenser applying experimental data obtained from the literature. For this purpose, a calculation code has been developed to determine the total heat transfer area of the heat exchanger. Therefore, we present a comparison between calculated and experimental results obtained from the literature. This comparison allowed the validation of the calculation method by applying the same experimental conditions. The discussion of the results indicates that we cannot use the ambient air in free convection mode as a cooling fluid if its temperature exceeds 30°C. This problem presents the greatest obstacle especially in the Saharan regions, such as in Biskra, where the average ambient air temperature during the summer exceeds 35°C. As a solution, we propose in this article the improvement of the heat transfer by the air-forced convection mode. Thus, it is established that the use of the air fan can extend the operating temperature limits of the condenser above 35°C.

© 2016 The authors. Published by the Faculty of Sciences & Technology, University of Biskra. This is an open access article under the CC BY license.

1. Introduction

Algeria has significant solar energy able to supply the global economy. It should be noted that Algeria has the largest proportion of the solar energy in the Mediterranean basin estimated at four times of the overall global energy consumption (Labeled 2012). It is therefore important to exploit this free and non-polluting resource in the field of the production of cold, particularly in isolated rural areas where conventional electrical grids are faulty.

The cooling machine investigated in this paper is a solar powered adsorption refrigerator. This machine seems a promising way to improve the living conditions in environmental and economic point of view. Several works in the field of adsorption refrigeration were performed by our research group (Rouag et al. 2014a; Labeled et al. 2015a).

The main heat exchangers of the solar refrigerating machine are the adsorber-collector, the condenser and the evaporator (Errougani 2007). It is obvious that the ultimate success of these systems depends largely on good study, design and realization of these exchangers. The thermal calculation of the condensers is very complicated, and essentially amounts to the wide diversity and the complexity of these technological devices: tubular condensers, plate condensers, air-cooled, water-cooled... (Aoues et al. 2011; Rouag et al. 2014b; Labeled et al. 2015b).

In this paper, we studied the condenser of solar adsorption refrigerator, which is the most sensitive element to the external factors as the ambient air temperature and the wind velocity. Several criteria are considered for the design of a condenser according to its use. The thermal power is still the main considered criterion, but the final choice of the device may depend on other parameters such as: heat transfer area, wall temperature, materials ... etc (Labeled 2012).

There are mainly two types of methods to calculate the condenser area: the numerical methods as the finite volume method and the overall analytical methods as NUT and LMTD methods (Rouag et al. 2014a).

In this work we studied the design of a finned tubes condenser of a solar adsorption refrigerator which will be tested in the region of Biskra. A calculation program code based on LMTD method is presented and validated with experimental data obtained from the literature (Errougani 2007; Lemmini et al. 2002; Lemmini and Errougani 2005, 2007). We have also studied the improvement of the heat transfer by the ambient air-forced convection regime.

2. System description

The studied system is based on the prototype of an intermittent activated carbon/methanol refrigerator, as shown in Figure 1. This solar adsorption refrigerator is mainly constituted of a collector, containing the adsorbent, connected to a condenser

✉ Corresponding author. E-mail address: rouagamar@yahoo.com

Nomenclature

| | |
|----------------------|--|
| <i>A</i> | longitudinal tube pitch |
| <i>A_o</i> | Heat transfer Area, m ² |
| <i>B</i> | transverse tube pitch |
| <i>C_p</i> | Specific heat, W kg ⁻¹ K ⁻¹ |
| <i>D</i> | diameter of tube, m |
| <i>g</i> | Gravity, m s ⁻² |
| <i>H</i> | Enthalpy, J kg ⁻¹ |
| <i>h</i> | Convective heat transfer Coefficient, W m ⁻² K ⁻¹ |
| <i>J</i> | Coburn factor |
| <i>U</i> | Overall heat transfer coefficient, W m ⁻² K ⁻¹ |
| <i>L</i> | Tube length / latent heat, m |
| <i>L_c</i> | Latent heat of condensation of the methanol ΔH |
| <i>LMTD</i> | log mean temperature difference |
| <i>ṁ</i> | Refrigerant mass flow rate, Kg s ⁻¹ |
| <i>N</i> | number of tube row |
| <i>F</i> | Correction factor $F = (\Delta T_{ML} - \Delta T_o) / (\Delta T_i - \Delta T_o)$ |
| <i>P1, P2</i> | Correlation parameters |
| <i>R</i> | fouling resistance, m ² K W ⁻¹ |
| <i>S_f</i> | Spacing between the fins, m |
| <i>T</i> | Temperature, °C |
| <i>t</i> | Time, s |
| <i>S</i> | finned surface per meter of length, m ² m ⁻¹ |
| <i>V</i> | Volume, m ³ |

Greek symbols

| | |
|-----------|---|
| μ | Dynamic viscosity, Pas |
| γ | Efficiency of the condenser, - |
| λ | Thermal conductivity, W m ⁻¹ K ⁻¹ |
| ρ | Density, kg m ⁻³ |
| β | Coefficient of expansion of the fluid, K ⁻¹ |
| ν | kinematic viscosity, m ² s ⁻¹ |

Subscripts

| | |
|------------|------------------|
| <i>a</i> | Air |
| <i>ai</i> | Air inlet |
| <i>ao</i> | Air outlet |
| <i>c</i> | Condensation |
| <i>e</i> | External |
| <i>h</i> | Hydraulic |
| <i>l</i> | Liquid |
| <i>i</i> | Internal |
| <i>LM</i> | logarithmic mean |
| <i>m</i> | Mean |
| <i>w</i> | Wall |
| <i>stm</i> | Steam |
| Δ | Difference |

and a refrigerating chamber contains the evaporator. Three valves between: adsorber-condenser, condenser-evaporator and evaporator-adsorber.

The refrigerator operates on a solar thermal adsorption cycle. The cycle can be divided into four basic sequential phases in a Clapeyron diagram. Figure 2 represents the evolution of the state of mixture adsorbent/adsorbate contained in the adsorber. The Phase (1-2) is the isosteric heating. In this phase, the solar radiation heats the collector-adsorber, containing the adsorbent, which provides the increasing of the pressure and temperature.

When the collector reaches the saturation pressure corresponding to the condensation temperature, the adsorbate vapor desorbed and passes to the condenser (condensation phase 2-3). When the sunlight decreases, the temperature of the collector decreases (phase 3-4).

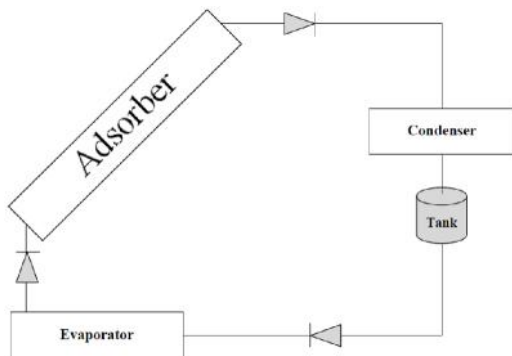


Fig. 1. Schematic representation of a solar adsorption refrigeration machine.

In this case, the pressure decreases to achieve to the same pressure of the evaporator. Cooling could start by opening the louver in the rear face of the collector/adsorber (isosteric cooling), this is the phase in which the cold is produced. The temperature and pressure has decreased, the adsorbent is physically in disequilibrium and will "recharge" by adsorbing the methanol contained in the evaporator. This steam is generated by the evaporation of the liquid in the evaporator (phase 4-1). This phase is produced by the latent heat of evaporation of methanol (Rouag et al. 2014a).

The condenser is a thermal unit; his role is to ensure the passage of the fluid from a gas (vapor) state to the liquid state. The main problem consists in defining the sufficient heat transfer area between the two fluids to transfer the needed heat quantity in a given configuration. The quantity of heat transferred depends on

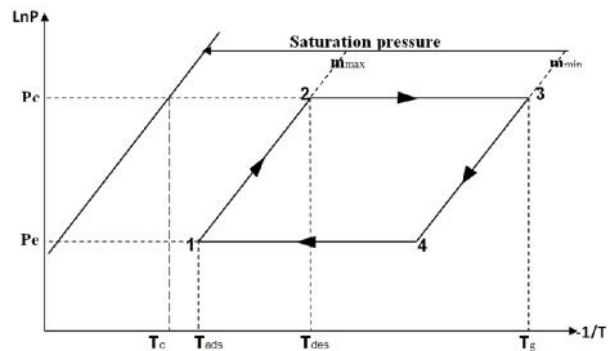


Fig. 2. Thermodynamic cycle of the adsorption refrigeration system illustrated on Clapeyron diagram.

the heat transfer area between the two fluids and on many other parameters as the thermal properties of fluids (specific heat, viscosity, thermal conductivity ...) and the convective-exchange coefficients.

The air condenser that we are studying is illustrated in Figure 3. It consists of a system of tubes with square fins. The refrigerant (methanol CH₃OH) flows freely in the tube and the ambient air ensures the condensation of the refrigerant vapor flowing out the tubes in natural convection mode.

3. Thermal design calculations

As mentioned above, the LMTD method is used to define the sufficient heat transfer area between the two fluids. This method needs an experimental database to find the parameters used for the calculation of the heat transfer coefficients. LMTD method uses three steps to calculate the heat transfer area of the condenser (Saunders 1988):

- Input of the necessary data: geometric data and physical properties of fluids.
- Thermal phase comprising geometric calculations (section, diameter, length ...). Then the heat transfer calculations.
- Results in summary form (heat power, exchange area...) or more detailed form (local value transfer coefficients, dimensionless characteristic numbers...).

The optimum heat and mass transfer area is then determined iteratively via the use of the final iterated value of the overall heat transfer coefficient. The final iterated value of the optimum heat and mass transfer area is obtained after a few iterations. Starting firstly by selecting the type of the condenser and then spend to the phase of thermal design to calculate the heat transfer area. The geometric optimization leading to decrease the transfer area with the same thermal efficiency and the sizing calculation of the condenser must be able to solve this problem.

The overheating of the air in the finned tubes heat exchangers (condenser) is generally given in (5 and 6 °C) in the case of natural convection (Rapin and Jacquard 1992). Unfortunately, the air has a very low specific heat capacity which decreases the overall heat transfer coefficient between vapour and condensed gas.

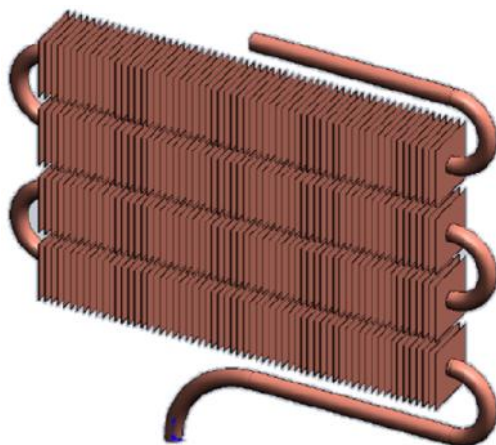


Fig. 3. Finned tubes air condenser.

Thus limits the use of the air in small installation like household cabinets or similar devices. To calculate the total heat transfer area required for methanol condensation, we introduce the geometric data and the thermo-physical characteristics for each fluid in the code by taking into account the ambient and the condensing temperatures (Fig. 4).

The following assumptions were considered for the calculation of air-cooled condensers:

- Stationary operating regime;
- Constant overall heat transfer coefficient (Kern 1951);
- Low flow rates (compressibility effects are negligible).

Heat transfer between the two fluids, from the outside to the inside of the condenser, is related to: (i) external convective heat transfer coefficient h_e : natural convection between the air and the external wall, (ii) thermal conductivity λ : conduction through the wall, (iii) internal convective heat transfer coefficient h_i : condensation of the methanol on the internal wall.

The simplified sequential steps of LMTD method to design the finned tubes condenser can be presented as follows:

3.1 External convective heat transfer coefficient

The air-side heat transfer coefficient h_e is calculated according to the geometry of the heat exchanger by the following equation:

$$h_e = \frac{Nu \rho_{methanol}}{D_e} \tag{1}$$

The Nusselt number in free convection can be calculated from the following correlation (Kern 1951):

$$Nu = 0.201 \left(Gr Pr \frac{S_f}{D_m} \right)^{\frac{1}{3}} \tag{2}$$

Where $S_f = 2.71 \left[\frac{s(T_p - T_{ae})g}{r \epsilon A} \right]^{-\frac{1}{4}}$ is the spacing between fins (Incropera and DeWitt 1985).

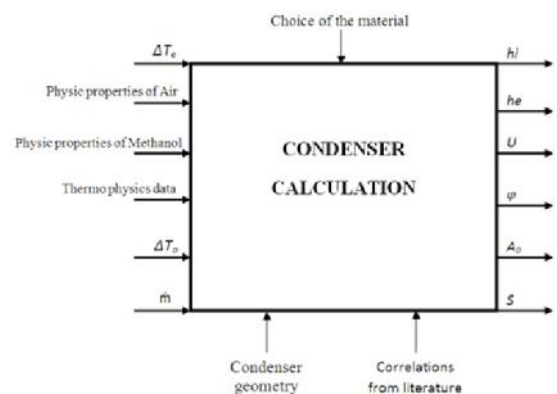


Fig. 4. Input/output parameters used in the condenser calculation code.

3.2. Internal convective heat transfer coefficient

The condensation is dominated by natural convection and laminar flow is encountered when Reynolds number of the vapour flow rate in smooth horizontal tubes is less than 35000 (Dobson and Chato 1998), which is the case in the present study. The internal heat transfer coefficient h_i during the condensation is determined by the following relation:

$$h_i = 0.555 \left[\frac{(\dots) g^3 L_c}{\dots (T_c - T_w) d_i} \right]^{\frac{1}{4}} \quad (3)$$

3.3. Overall heat transfer coefficient

The overall heat transfer coefficient U , based on the external transfer area, is given by Eq. (4) (Kern 1951):

$$U = \frac{1}{\frac{1}{y_g h_e} + R_o + R_w \frac{S_e}{S_m} + \left(R_i + \frac{1}{h_i} \right) \frac{S_e}{S_i}} \quad (4)$$

The optimum heat and mass transfer area can then be calculated using Eq. (5) (Rapin and Jacquard 1992):

$$A_0 = \frac{\{ \dots \}}{F U \Delta T_{ML}} \quad (5)$$

The heat flow rate is the mass flow rate times the latent heat of condensation L_c of the methanol (Dobson and Chato 1998):

$$\{ \dots \} = \dot{m} L_c \quad (6)$$

Where the mass flow rate \dot{m} is calculated by following expression:

$$\dot{m} = \dots V / t \quad (7)$$

The log mean temperature difference ΔT_{ML} in the condenser is defined by the following relation (Rapin and Jacquard 1992):

$$\Delta T_{ML} = \frac{(T_c - T_{ai}) - (T_c - T_{ao})}{\log \left(\frac{T_c - T_{ai}}{T_c - T_{ao}} \right)} \quad (8)$$

T_{ao} and T_{ai} are the air temperatures, outlet and inlet respectively, and T_c is the condensation temperature. The correction factor F applied to LMTD is defined according to the heat exchanger geometry (Rapin and Jacquard 1992).

We can calculate the outlet air temperature in the condenser by the Eq. (9):

$$T_{ao} = T_{ai} + \{ \dots \} / (h_e y_g A_0) \quad (9)$$

4. Results and Discussion

4.1. Natural convection regime

To validate the calculation code, we use the same experimental data of Errougani (2007) which are: the ambient temperature, the condenser temperature, material (copper) and the same heat and mass transfer area (7.5 m²) for March (14 to 26) sequence

(Lemmini et al. 2002; Lemmini and Errougani 2005) and April (02 to 15) sequence (Lemmini and Errougani 2007). However, the authors report that there is a lack of measures on 6 April 2004 only due to technical problems related to the acquisition chain.

Table 1 shows the evolutions of the ambient temperature, the average temperature of the condenser and the calculated values of the required total heat transfer area for the two sequences of the experimental results. The difference between the average temperature of the condenser and the ambient temperature can reach 12 °C during the desorption phase. This difference, which depends on the desorbed quantity of methanol and the climatic conditions, is important to estimate the total heat transfer area required for condensation.

The calculated values of the required total heat transfer area shown in Figures 5a and 5b. According to Lemmini and Errougani, the condensation took place almost during all days. Authors report also that there is no condensation of methanol vapour in the days of 8th and 9th of April. In these two days, weather was cloudy which makes the temperature gap between the two fluids (air and methanol) near zero. This temperature gap is inversely proportional to the total heat transfer area of the condenser (Eq. 5) which means that the methanol needs a large heat transfer area for the condensation process. In this case, the heat transfer area is estimated more than 7.5 m² (nearly 27 m²) as shown in figure 5b. The same problem also occurred in 26th of March (Fig. 5a). As a solution of this problem, we can think to

Table 1. Calculated values of the required total heat transfer area for the two sequences of experimental results obtained by Errougani 2007; Lemmini et al. 2002; Lemmini and Errougani 2005, 2007.

| | Day (2004) | T _{amb} (mean-day) From 10 to 18h | T _c [°C] | A ₀ [m ²] |
|----------------|------------|---|---------------------|----------------------------------|
| March sequence | March 14 | 14 | 24 | 4.32 |
| | March 15 | 16 | 28 | 3.03 |
| | March 16 | 18 | 28 | 4.32 |
| | March 17 | 19 | 27 | 7.43 |
| | March 18 | 17 | 27 | 4.34 |
| | March 19 | 17.5 | 27 | 4.82 |
| | March 20 | 22 | 28 | 7.08 |
| | March 21 | 17 | 27.5 | 3.91 |
| | March 22 | 16.5 | 27.5 | 3.57 |
| | March 23 | 15 | 27 | 3.03 |
| | March 24 | 14 | 24 | 4.35 |
| March 25 | 20 | 31 | 3.56 | |
| March 26 | 14 | 17 | 16.61 | |
| April sequence | April 02 | 16.5 | 27 | 3.91 |
| | April 03 | 17 | 26 | 5.46 |
| | April 04 | 18.5 | 26.5 | 7.43 |
| | April 05 | 25 | 32 | 8.10 |
| | April 07 | 22 | 34 | 3.02 |
| | April 08 | 20 | 22 | 27.29 |
| | April 09 | 17 | 19 | 27.29 |
| | April 10 | 18 | 27 | 5.46 |
| | April 11 | 17.5 | 25.5 | 5.90 |
| | April 12 | 17 | 24 | 8.12 |
| | April 13 | 20 | 26 | 8.97 |
| | April 14 | 18 | 26 | 5.89 |

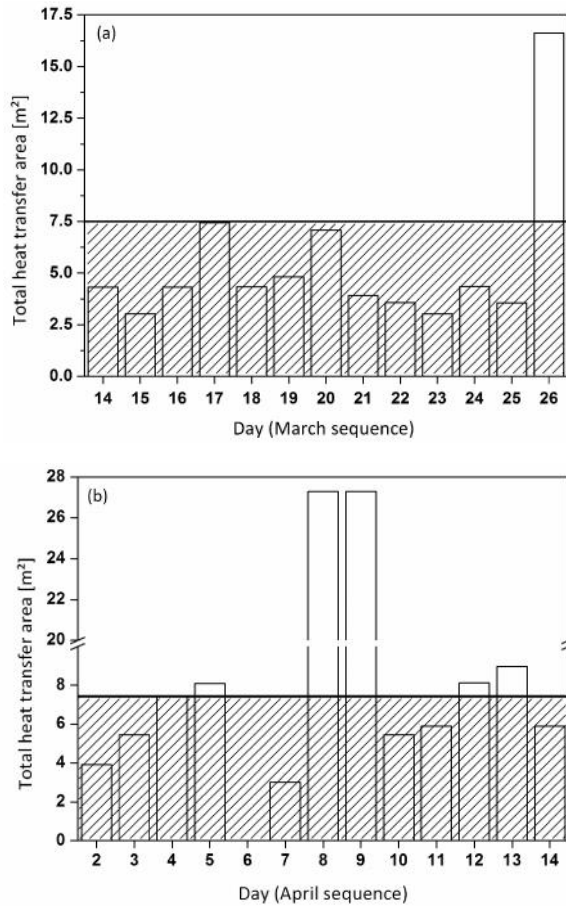


Fig. 5. Comparison of the calculated heat transfer area of the condenser, in *natural convection*, with the area used in the experimental device of Errougani and Lemmini (7.5 m²): a) March sequence & b) April sequence.

increase the heat transfer area of the condenser. This proposal, costly and makes the condenser very bulky, is a not-convenient solution to ensure the condensation of methanol vapour. We can find in the literature several proposals to avoid this problem such as the integration of water spray systems, which is also a not-practical solution in Saharan regions. For that, we propose in the following subsection the use of an electric fan, with low power consumption, connected to a photovoltaic panel.

4.1. Forced convection regime

As the previous subsection, we use the experimental results of Lemmini and Errougani cited above. The only difference is that we have supplied the condenser with an electrical fan with 2 ms⁻¹ of velocity. Wang et al. (2000) propose a correlation for finned tubes heat exchanger having plain geometry for the forced convection for different number of tube rows *N*.

$$h_e = j \dots_a C p_a V_a Pr^{-2/3} \tag{10}$$

For *N* = 1:

$$j = 0.108(Re^{-0.29}) \left(\frac{A}{B}\right)^{P1} \left(\frac{S}{De}\right)^{-1.084} \left(\frac{S}{D_h}\right)^{-0.786} \left(\frac{S}{A}\right)^{P2} \tag{11}$$

With *P1* = 1.9 – 0.23 *Log*(*Re*) and *P2* = –0.236 + 0.126 *Log*(*Re*)

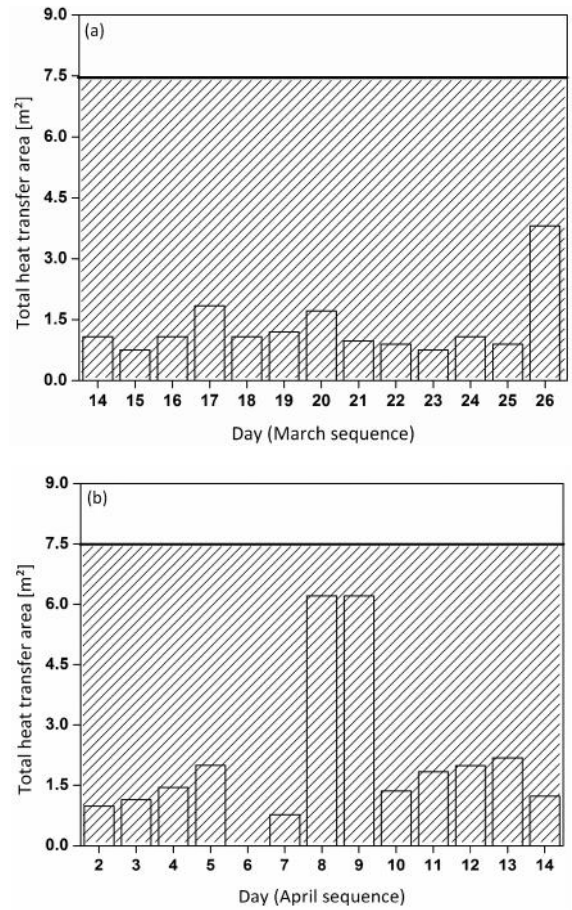


Fig. 6. Comparison of the calculated heat transfer area of the condenser, in *forced convection*, with the area used in the experimental device of Errougani and Lemmini (7.5 m²): a) March sequence & b) April sequence.

Figures 6a and 6b show the results of the required heat transfer area in forced convection compared to the area of the condenser used in the experimental device of Errougani and Lemmini (7.5 m²). According to these results and after comparison with natural convection regime (fig. 5), we can conclude that the forced convection regime presents a gain about 70 % of condenser area.

In Figures (7 and 8) the temperature of the ambient air is fixed at (15°C, 20°C, 25°C, 30°C and 35°C) and the condensation temperature is varied to see the influence of these two temperatures on the internal, external and overall heat transfer coefficients respectively.

Figure 7 gives the variation of the internal convective heat transfer coefficient *hi* versus the condensation temperature for different ambient air temperatures. The internal convective heat transfer coefficient (coefficient of condensation) decreases with the increasing of the condensation temperature. This coefficient reaches its highest values for the ambient air temperature equal to 15 °C. Furthermore, the internal heat transfer coefficient (figure 7) is higher than the external convective heat transfer coefficient in both natural and forced convection regimes (Figure 8a).

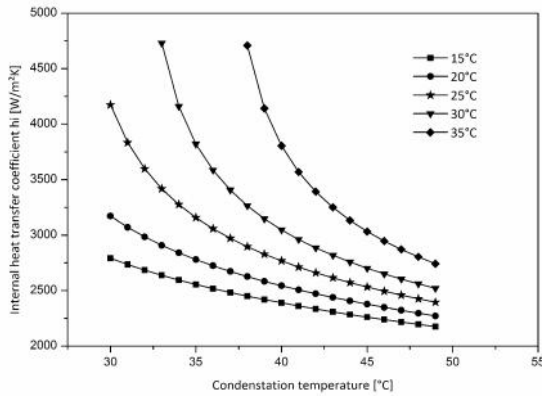


Fig. 7. Influence of the condensation temperature on the internal heat transfer coefficient.

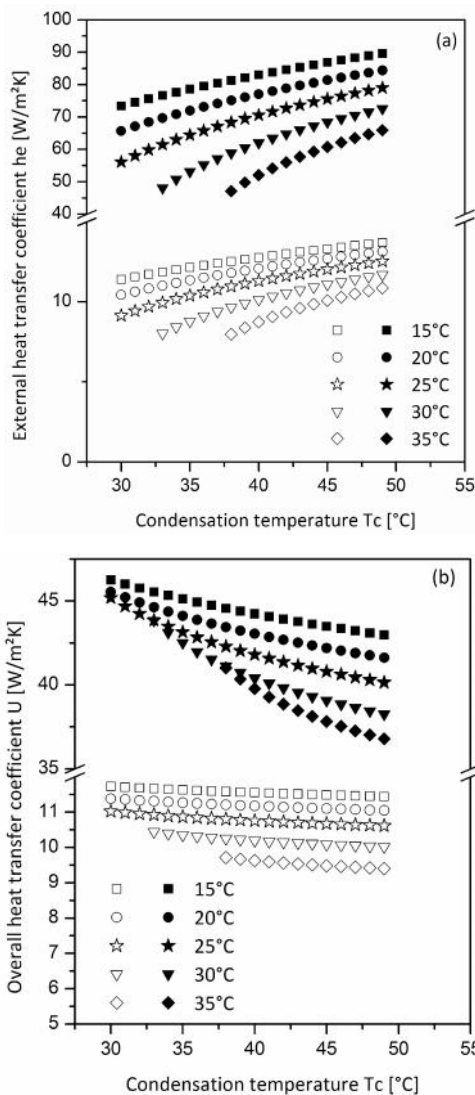


Fig. 8. Influence of the condensation temperature on: a) external convective heat transfer coefficient & a) overall heat transfer coefficient. Black symbols are for forced convection and white symbols for natural convection.

Figures 8a and 8b give the variation of the external h_e and the overall U heat transfer coefficients, respectively, versus the condensation temperature for the different ambient air

temperatures mentioned above in both flow regimes (natural and forced convection). In the case of natural convection, the external heat transfer coefficient varies proportionally with the condensation temperature (Fig. 8a). This coefficient takes the maximum values at the ambient air temperature of 15 °C. It decreases with the increasing of the ambient temperature and reaches around $6 \text{ W m}^{-2}\text{K}^{-1}$ for ambient temperatures greater than 30 °C. In this case, the heat exchange is very weak or almost non-existent and this is one of the disadvantages of the use of dry air as a cooling fluid.

The overall heat transfer coefficient U varies inversely with the increasing of the condensation temperature. At the ambient air temperature of 15 °C, the overall coefficient takes its highest values and continuing to decrease with the increasing of the ambient air temperature. The coefficient reaches less than $10 \text{ W m}^{-2}\text{K}^{-1}$ for the ambient temperature higher than 30 °C as shown in the Figure 8b.

Based on the above results, we can conclude that the cold production process, in the solar adsorption refrigerator, can be stopped with the free air condenser where the ambient temperature is higher than 30 °C. This can be explained why there are no experimental tests in the summer on the experimental setup of Errougani and Lemmini (Errougani 2007; Lemmini et al. 2002; Lemmini and Errougani 2005, 2007).

In the case of the forced convection regime, in the top side of figures 8a and 8b, the heat exchange is clearly improved by the external convective heat transfer coefficient h_e . In this case, the overall heat transfer coefficient $U (>35 \text{ W m}^{-2}\text{K}^{-1})$ is very enough to condense the methanol vapour. These results showed that the refrigerator can operate at temperatures higher than 35°C.

5. Conclusion

In this paper, a solar adsorption refrigerator with finned tube condenser driven by natural convection is investigated. The log mean temperature difference, LMTD, method is used to calculate the total heat transfer area. To design the condenser, the whole interior of the condenser is considered as one volume with two-phase region. Therefore only one overall heat transfer coefficient is considered.

The results obtained from the developed calculation code are validated by comparison with experimental data, obtained from the literature.

A parametric study is presented to show the influence of some parameters (the condensation temperature and ambient air temperature) on the total heat transfer area of the condenser. It was concluded that this type of heat exchangers is greatly affected by ambient air temperature which influences directly the quality of the heat transfer. This problem presents the greatest obstacle that could prevent using dry air as a cooling fluid especially in the Saharan regions, such as in Biskra, where the average ambient air temperature exceeds 35°C during the summer. To overcome this problem, we have proposed in this article the use of an electric fan connected to a photovoltaic

panel operates in hot times. It was established from the present conclusions that the refrigerator can operate at temperatures higher than 35 °C which encourages us to realize it in our laboratory in Biskra University. We can think also to couple the finned tube heat exchanger (condenser) with a shallow geothermal source. This will be the subject of another work in preparation.

Acknowledgments

This study was supported by the Algerian Ministry of Higher Education and Scientific Research as a part of CNEPRU project.

References

- Aoues, K., N. Moumami, M. Zellouf & A. Benchabane (2011) Thermal performance improvement of solar air flat plate collector: a theoretical analysis and an experimental study in Biskra. *International Journal of Ambient Energy* 32(2): 95-102.
- Dobson, M. & J. Chato (1998) Condensation in smooth horizontal tubes. *Journal of Heat Transfer* 120(1): 193-213.
- Errougani, A. (2007) Fabrication et expérimentation d'un réfrigérateur solaire à adsorption utilisant le couple charbon actif - méthanol dans le site de Rabat. Thèse de Doctorat, Faculté des sciences, Université Mohammed V, 128.
- Incropera, F. P. & D. P. DeWitt (1985) *Fundamentals of heat and mass transfer*: 2nd edition. New York, John Wiley & Sons.
- Kern, D. Q. (1951) *Process Heat Transfer*. New York, McGraw-Hill.
- Labeled, A. (2012) Contribution à l'étude des échanges convectifs en régime transitoire dans les capteurs solaires plans à air: Application au séchage des produits agro-alimentaires. Thèse de Doctorat, Université de Biskra.
- Labeled, A., A. Rouag, A. Benchabane, N. Moumami & M. Zerouali (2015a) Applicability of solar desiccant cooling systems in Algerian Sahara: Experimental investigation of flat plate collectors. *Journal of Applied Engineering Science & Technology* 1(2): 61-69.
- Labeled, A., N. Moumami, A. Benchabane & M. Zellouf (2015b) Experimental analysis of heat transfer in the flow channel duct of solar air heaters (SAHs). *International journal of heat and technology* 33 (3): 97-102.
- Lemmini, F. & A. Errougani (2005) Building and experimentation of a solar powered adsorption refrigerator. *Renewable Energy* 30(13): 1989-2003.
- Lemmini, F. & A. Errougani (2007) Experimentation of a solar adsorption refrigerator in Morocco. *Renewable Energy* 32(15): 2629-2641.
- Lemmini, F. & A. Errougani & F. Bentayeb (2002) Experimentation of an adsorptive solar refrigerator in Rabat. FIER' 2002, Tétouan - Maroc, 260-265.
- Rapin, P. J. & P. Jacquard (1992) *Installations frigorifiques; Tome 2, Technologie*: 6ème édition, Ivry-sur-Seine: PYC Edition.
- Rouag, A., A. Benchabane, N. Boultif & A. Labeled (2014a) Contribution to the design of the heat exchangers of a solar adsorption refrigerator: condenser sizing calculations. 13th International conference on clean energy ICCE, Istanbul, Turkey.
- Rouag, A., A. Benchabane, A. Labeled & N. Boultif (2014b) Use of shallow geothermal energy to improve the efficiency of air heat exchangers: Proposal of a Geothermal Air-Cooler (GAC). Patent N° 140719. National Algerian Institute for Industrial Property, INAPI. Algeria. 04-12-2014.
- Saunders, E.A.D. (1988) *Heat exchangers*. New York, John Wiley and Sons Inc.
- Wang, C. C., K. Y. Chi & C. J. Chang (2000) Heat transfer and friction characteristics of plain fin-and-tube heat exchangers, part II: Correlation. *International Journal of Heat and mass transfer* 43(15) 2693–2700.